CURRENT STATUS OF THE SCHOTTKY SENSOR SYSTEM AT THE CR AT FAIR

M. Hansli*, A. Penirschke, R. Jakoby, IMP, TU Darmstadt, Germany
Peter Hülsmann, Wolfgang Kaufmann, GSI, Darmstadt, Germany

Abstract

In this paper, the current status of the Schottky Cavity Sensor development for the Collector Ring (CR) at FAIR, a dedicated storage ring for secondary particles, rare isotopes, and antiprotons, is presented. Designed for longitudinal and transversal Schotty signals, the Sensor features a pillbox cavity with attached waveguide filters utilizing the TM_{010}-mode at 200 MHz for longitudinal and the TM_{110}-mode at around 330 MHz for transversal Schottky measurements. Separated coupling structures are used for mode-selective coupling to measure the different Schottky planes independently. A ceramic vacuum shielding inside the pillbox is introduced to allow for non-hermetic adjustable coupling and tuning devices as well as waveguide structures. Simulations of the structure are presented with focus on the influence of the coupling structures and the ceramic vacuum shielding. Measurements of a scaled demonstrator are compared to simulations.

INTRODUCTION

The collector ring at FAIR is a dedicated ring for accumulation of different particle species including antiprotons and heavy ions, as well as an isochronous mode for mass measurements. For the observation of Schottky signals at very low intensities a resonant structure was proposed [1, 2]. It consists of two pillbox like cavities with attached waveguide structures, one for each transversal plane. Longitudinal measurements are utilizing the TM_{010}-mode, called monopole mode in the following, while the TM_{110}-mode (dipole mode) is used for transversal measurements in one plane. At the center of the beampipe, the dipole mode is zero while the monopole mode has a maximum there, leading to a difference in excitation of around four orders of magnitude. As the bandwidth requirements from the Schottky spectra limit the Q of the cavity to around 180, an independent coupling to both modes minimizes the interference. A magnetic coupling loop at the zero-plane of the dipole mode is used to exclusively couple out the monopole mode. As there is no suitable position for an independent coupling to the dipole mode the attached waveguide structures are used as frequency selective coupling. By using the difference signals from both sides, the dipole mode can be extracted. To adapt to different revolution frequencies and frequency spreads, an adjustable coupling and adjustable perturbers will be used. A scaled demonstrator was realized to compare simulation results and measurements and investigate the behavior of the coupled resonator structures (Fig. 1).

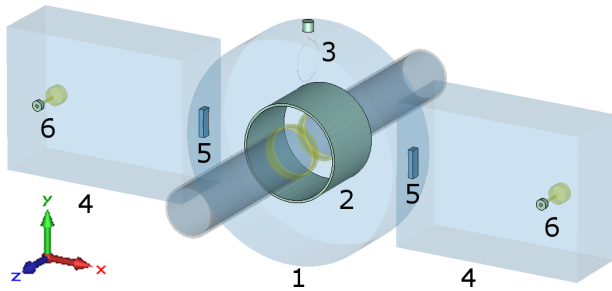

Figure 1: The proposed structure with E-field coupling pins: (1) pillbox cavity, (2) ceramic vacuum shielding, (3) coupling loop (4) waveguide structures (5) Coupling slots, (6) coaxial ports.

MEASUREMENTS OF THE DEMONSTRATOR

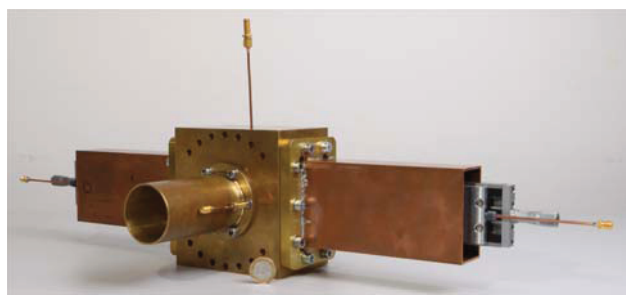

Figure 2: The realized demonstrator with movable shorts. The four ports are: magnetic loop coupling on top, short electric pin at the front and coupling loops at the shortening waveguides.

A simplified demonstrator (see Fig.2) without the ceramic shielding was built from brass in a split block technique at a scale of around 8.6 enabling the use of standard waveguides and flanges (S band, WR-284/WG10). The monopole mode frequency is 1.86 GHz and the dipole mode frequency 2.77 GHz at this scale. In addition to the coupling loop on top a weakly coupling electric pin is installed in the end plane to observe the dipole mode inside the cavity. Two different waveguide structures can be mounted at the sides, either movable waveguide shorts with coupling loops at the ends or pin coupled waveguides of

* hansli@imp.tu-darmstadt.de

ISBN 978-3-95450-127-4

fixed length. Aim of the movable waveguide shorts is to find the optimum length and investigate the interaction between the three resonant structures. They consist of fitted aluminum blocks which where fitted into the waveguides and can be moved by a manual linear unit. Semi rigid coaxial cables are routed through the middle of the block ending with an magnetic coupling loop each.

Measurements of the Movable Waveguide Shorts

The movable waveguide shorts where connected directly, without the cavity, to investigate the two different loop sizes. Figure 3 depicts the measured transmission coefficient. From Tab.1 can be seen, that the strong coupling of the big loops is lowering the third mode around 13.4% while using small loops is leading to the frequencies up to 0.4% higher than the analytic solution. Furthermore, the transmission coefficient for the big loop still shows a strong frequency dependence above the cutoff demonstrating the importance of the length of the waveguide structure to the overall sensor performance.

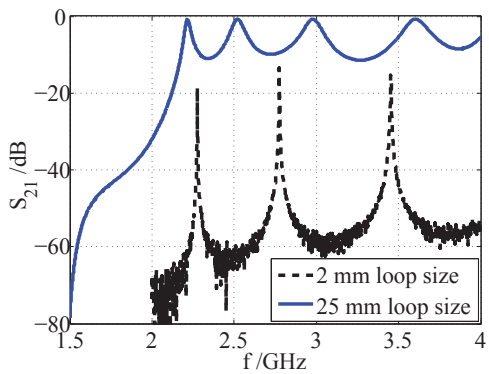

Figure 3: Transmission measurement of the movable waveguide shorts in a back-2-back setup with a length of 164 mm, (black curve starts at 2 GHz).

Table 1: Comparison of Measured and Calculated Resonance Frequencies

Mode	analytic	Loops 2 mm	Loops 25 mm
1	2.270 GHz	2.276 GHz	2.216 GHz
2	2.768 GHz	2.775 GHz	2.521 GHz
3	3.440 GHz	3.454 GHz	2,980 GHz

S-Parameter Measurements of the Demonstrator

The interaction of the three resonant structures where investigated with a 4-port Vector Network Analyzer. Figure 4 shows the S_{34}-Parameter, the transmission from one waveguide short to the other. With the coupling slots in the cavity walls of 23 mm × 2 mm, the measurement shows three peaks. The position of the peaks can be changed by varying the length of the shorts. However, if the resonances of the waveguide shorts are to close in frequency to the cavity mode a clear attribution to the peaks is not possible anymore. By tuning one waveguide short, all three peaks are moving. Figure 4 shows the setting with the smallest distance between the peaks. Using the bigger loops, the 2 waveguide resonance peaks in the transmission are not observable anymore, although the level of the transmission is affected by the position of the short. The system was modeled as a parallel RLC-circuit with attached transmission lines in AWR Design Enviroment [3] and fitted to the measurements. It can be seen, that the coupling between the cavity RLC-circuit and the waveguides is determining the minimal frequency distance that can be achieved.

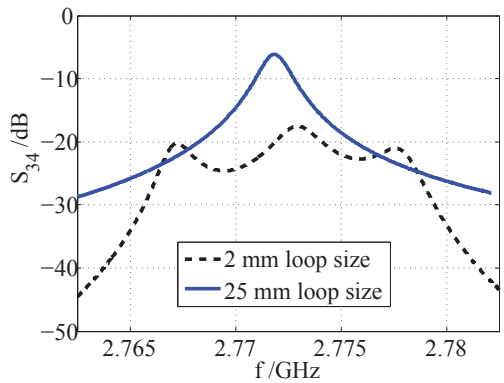

Figure 4: S-Parameter measurement of the demonstrator. Transmission from waveguide structure to waveguide structure (see Fig. 2).

Perturbation Measurements

To determine the field distribution inside the cavity, an automated perturbation measurement [4] was performed, using linear units to move the sensor and the perturber, a 20 cm long alumina tube with diameter of 1 mm on a fishing line. The long tube does not allow spacial resolution along the longitudinal axis but gives the integration along its length instead, which is the relevant parameter for the coupling between the particles and the beam. The S_{34}-Parameter was measured for different positions of the perturber on the horizontal plane, centered vertically and longitudinally. The resonance frequencies where extracted utilizing a fitting. The distribution of the electric field strength E is extracted according to

$$\frac{f^2 - f_0^2}{f^2} \propto -\chi E^2, \qquad (1)$$

with χ beeing a constant depending on the perturber. To compare the result with simulations, an Eigenmode-simulation was conducted with CST STUDIO SUITE®and the electric field was integrated along a longitudinal path, neglecting the thickness of the perturber. The results where normalized to see the qualitative distribution.

ISBN 978-3-95450-127-4

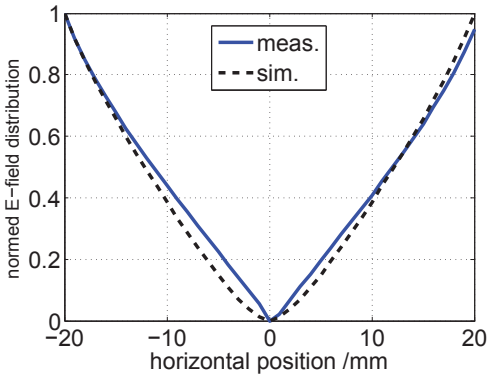

Figure 5: Normalized frequency deviation from the pertubation measurements versus simulated integrated field distribution.

STATUS OF THE SIMULATIONS

For the different use cases of the CR revolution frequency and frequency spread are varying. To maintain optimum performance, especially for the observation of very small intensity beams, adjustable coupling and movable perturbers are foreseen. These structures, as well as the rectangular waveguide structures are much easier to fabricate and operate in an non-hermetic environment. Therefore a ceramic pipe is introduced as a vacuum shielding, as depicted in Fig.1. In Table 2, the influence of the pipe on the R/Q value, the frequency of the dipole mode and the radius of the cavity are shown, as simulated with CST STUDIO SUITE®. To maintain the 200 MHz monopole mode frequency the radius varies from 55.17 cm without shielding to 47.68 cm for alumina with 15 cm radius. It can be seen, that the R/Q values are increased by the ceramic at the expense of an rising dipole mode frequency. As a trade-off, the shielding was chosen to be alumina with a radius of 20 cm, keeping the frequency at 330 MHz. For this selection, the influence of the gap geometry was investigated by simulating the pillbox without attached waveguide structures to save simulation time. The results in Tab.3 show a strong impact on the dipole frequency without identifying an optimal configuration. Therefore, the gap is set to 20 cm $\times$ 1 cm to keep the dipole mode at 330 MHz.

CONCLUSION AND OUTLOOK

For the proposed Schottky sensor, a demonstrator was realized and measured with different methods. Measurements of the movable waveguide shorts have shown the influence of the length on the coupling strength and estimated the achievable levels. For the extraction of the dipole mode the transition from the waveguide to the cables is important to avoid having the three resonance peaks. The sensor design was upgraded with a ceramic vacuum shielding to allow for non-hermetic environment outside the inner cavity. The influence of the ceramic onto the sensor was investigated. Following the results, a vacuum shielding with a 20 cm radius was chosen made from alumina. The gap dimensions of 20 cm$\times$1 cm result in a good trade-off between R/Q-value and dipole mode frequency.

Table 2: R/Q for Different Radii of the Vacuum Window, for 200 MHz Monopole Mode at a Coupling Slot of 2 cm$\times$23 cm

Window		R/Q (offset/cm) /Ω			Dipole
ϵ_r	r/cm	Mono.	Di. (1)	Di. (5)	f_r/MHz
4	15	175,51	0,44	11,07	341,20
4	20	170,46	0,40	10,12	335,38
4	25	166,86	0,36	8,98	329,65
4	30	165,88	0,33	8,16	325,74
9,6	15	171,93	0,61	15,87	347,92
9,6	20	159,46	0,47	11,67	330,55
9,6	25	154,13	0,35	8,77	318,09
9,6	30	151,76	0,28	7,09	311,17
4	cone	184,88	0,5	12,78	349,05
9,6	cone	188,94	1,05	26,31	371,07
1		173,74	0,34	8,57	333,07

Table 3: Comparison of Different Gap Geometries for a Vacuum Shielding of 20 cm Without Waveguides

Gap		Cavity	f/MHz	R/Q/Ω(offs. /cm)		
l	h	r	Dipole	Mono.	Di.(1)	Di(5)
5	1	34.88	428.07	157.67	0.55	13.75
5	2	30.56	456.18	138.65	0.77	19.26
5	3	29.39	453.06	123.36	0.79	19.75
10	1	35.27	419.86	174.65	0.63	15.66
10	2	39.24	389.93	163.67	0.56	14.07
10	3	38.15	394.89	154.19	0.63	15.68
15	1	45.30	348.85	168.56	0.47	11.66
15	2	44.50	353.91	164.98	0.50	12.61
15	3	43.78	357.88	160.53	0.54	13.57
20	1	48.04	330.75	159.20	0.46	11.59
20	2	47.61	333.48	158.24	0.48	12.07
20	3	47.22	335.78	156.66	0.50	12.56
25	1	49.59	320.00	149.90	0.46	11.58
25	2	49.42	321.14	149.95	0.47	11.76
25	3	49.27	322.14	149.68	0.48	11.95

REFERENCES

[1] M. Hansli et al., "Conceptual Design of a High Sensitive Versatile Schottky Sensor for Longitudinal and Transversal Schottky for the CR at FAIR", Proceedings of DIPAC 2011

[2] M. Hansli et al., "Investigations on High Sensitive Sensor Cavity for Longitudinal and Transversal Schottky for the CR at FAIR", Proceedings of IPAC 2011

[3] AWR, `http://www.awrcorp.com/products/microwave-office`

[4] Leonard C. Maier, "Field Strength Measurements in Resonant Cavities", Technical Report No. 143, Research Laboratory of Electronics, MIT, (1949)

ISBN 978-3-95450-127-4